coated SiN lines corresponds to voids at SiN-polymer interfaces (i.e., voiding underneath the contact). The contrast is due to the distinct viscoelastic response from the specimen acoustic wave from the voids. Interestingly, a notable hardening of the polymer in the trench and its sidewall is also evident in the phase image, which results from thermal annealing and possibly poor adhesion with SOD. Because it is nondestructive, SNFUH may be an ideal toolset for such subsurface metrology needs.

The efficacy of SNFUH in imaging of embedded or buried substructures in biology is demonstrated in Fig. 4, which depicts high resolution and remarkably high contrast arising from malaria parasites inside infected red blood cells (RBCs). The details of in vitro infection by malaria parasites are reported in (*30*); here, we demonstrate early-stage direct and real-space in vitro imaging of the presence of parasites inside RBCs without any labels or sectioning of cells, and under physiologically viable conditions. *Plasmodium falciparum* strain 3D7 was cultured in vitro by a modification of the method of Haldar *et al*. (*31*). Parasites were synchronized to within 4 hours by a combination of Percoll purification and sorbitol treatments, cultured to 10% parasitemia, and harvested at the indicated times.

SNFUH imaging was performed using the near-contact mode method for imaging soft structures. The SNFUH electronic module was used to bring the cantilever into near-contact mode, and then the sample was scanned over the RBCs while maintaining the near-field regime. An AFM topography image and a SNFUH phase image from infected RBCs are shown in Fig. 4, A and B, respectively. As expected, the AFM topography image shows the typical surface morphology of an infected RBC, whereas the SNFUH phase image shows remarkably high contrast from the parasite residing well inside the RBC. In addition to several other features reminiscent of membrane proteins and subcellular contents, multiple parasites are clearly evident. The morphology, spatial scale, and distribution of parasites are consistent with prior accounts of such infection (*30*, *32*). To further demonstrate the capability of SNFUH for early-stage diagnosis of parasite infection, we examined RBCs incubated for only 4 hours; infection after such a brief period is difficult to validate by other noninvasive techniques such as fluorescence tagging. The images in Fig. 4, C and D, show that SNFUH is sensitive to early-stage parasite infection in RBCs, as reflected by image contrast consistent with parasite infection.

These representative examples of SNFUH development and applications demonstrate a versatile toolset for nondestructive, high-resolution, real-space imaging of diverse materials systems. We believe the SNFUH approach fills the critical gap in spatial resolution at the 10- to 100-nm scale for nondestructive subsurface imaging in physical sciences, engineered systems, and biology.

References and Notes

1. H. N. Lin, *Appl. Phys. Lett.* **74**, 2785 (1999).
2. M. R. VanLandingham *et al*., in *Interfacial Engineering for Optimized Properties*, C. L. Briant, C. B. Carter, E. L. Hall, Eds., vol. 458 of *Materials Research Society Proceedings* (Materials Research Society, Pittsburgh, PA, 1997), pp. 313–318.
3. M. R. VanLandingham *et al.*, *J. Adhesion* **64**, 31 (1997).
4. B. Bhushan, L. Huiwen, *Nanotechnology* **15**, 1785 (2004).
5. M. R. VanLandingham *et al.*, *J. Mater. Sci. Lett.* **16**, 117 (1997).
6. K. Inagaki, G. A. D. Briggs, O. B. Wright, *Appl. Phys. Lett.* **76**, 1836 (2000).
7. G. A. D. Briggs, *Acoustic Microscopy* (Clarendon, Oxford, 1992), p. 33.
8. T. M. Nelson, R. W. Smith, *Adv. Mater. Process.* **162**, 29 (2004).
9. G. S. Shekhawat *et al.*, *Appl. Phys. Lett.* **68**, 779 (1996).
10. C. F. Quate, *Surf. Sci.* **299–300**, 980 (1994).
11. W. Dickson, S. Takahashi, R. Polland, R. Atkinson, *IEEE Trans. Nanotechnol.* **4**, 229 (2005).
12. K. Lindfors, M. Kapulainen, R. Ryytty, M. Kaivola, *Opt. Laser Technol.* **36**, 651 (2004).
13. B. C. Larson, W. Yang, G. E. Ice, J. D. Budai, J. Z. Tischler, *Nature* **415**, 887 (2002).
14. X. Wang, Y. J. Pang, G. Ku, G. Stoica, L. H. V. Wang, *Opt. Lett.* **28**, 1739 (2003).
15. K. Kostli, P. C. Beard, *Appl. Opt.* **42**, 1899 (2003).
16. D.-Z. Huang, J.-B. Li, Z. Sheng, *Chin. J. Med. Imaging Technol.* **20**, 1815 (2004).
17. International Technology Roadmap for Semiconductors (http://public.itrs.net).
18. B. Altemus, G. S. Shekhawat, R. Geer, B. Xu, J. Castracane, *Proc. SPIE 4558* (2001).
19. R. E. Geer, O. V. Kolosov, G. A. D. Briggs, G. S. Shekhawat, *J. Appl. Phys.* **91**, 4549 (2002).
20. O. Kolosov, R. M. Castell, C. D. Marsh, G. A. D. Briggs, *Phys. Rev. Lett.* **81**, 1046 (1998).
21. D. C. Hurley, K. Shen, N. M. Jennett, J. A. Turner, *J. Appl. Phys.* **94**, 2347 (2003).
22. O. Hirotsugu, T. Jiayong, T. Toyokazu, H. Masahiko, *Appl. Phys. Lett.* **83**, 464 (2003).
23. L. Muthuswami, R. E. Geer, *Appl. Phys. Lett.* **84**, 5082 (2004).
24. M. T. Cuberes, H. E. Assender, G. A. D. Briggs, O. V. Kolosov, *J. Phys. D* **33**, 2347 (2000).
25. L. Cheng, P. Fenter, M. J. Bedzyk, N. C. Sturchio, *Phys. Rev. Lett.* **90**, 255503-1-4 (2003).
26. B. P. Tinkham, D. A. Walko, M. J. Bedzyk, *Phys. Rev. B* **67**, 035404-1-6 (2003).
27. K. Shull, A. Kellock, *J. Polym. Sci. B* **33**, 1417 (1995).
28. E. T. Ogama *et al.*, *IEEE International Reliability Physics Symposium, 40th Annual Proceedings* (IEEE, Piscataway, NJ, 2002), pp. 312–321.
29. R. R. Keller, C. E. Kalnas, J. M. Phelps, *J. Appl. Phys.* **86**, 1167 (1999).
30. E. Nagao, O. Kaneko, J. A. Dvorak, *J. Struct. Biol.* **130**, 34 (2000).
31. K. Haldar, M. A. Ferguson, *J. Biol. Chem.* **260**, 4969 (1985).
32. D. Gaur, D. C. Ghislaine, L. H. Miller, *Int. J. Parasitol.* **34**, 1413 (2004).

33. Supported by NSF Major Research Instrumentation grant DMR-0420923, NSF Nanoscale Science and Engineering Center grant EEC-0118025, and based on U.S. Department of Energy Basic Energy Sciences grant DE-FG02-92ER45475. This work made use of the NU*ANCE* center facilities at Northwestern University. We thank K. Shull and A. Hagman for polymer-nanoparticle samples, and K. Haldar and her group for assistance with the malaria-infected RBCs.

20 July 2005; accepted 22 August 2005
10.1126/science.1117694

A 5-Micron-Bright Spot on Titan: Evidence for Surface Diversity

Jason W. Barnes,[1]* Robert H. Brown,[1] Elizabeth P. Turtle,[1] Alfred S. McEwen,[1] Ralph D. Lorenz,[1] Michael Janssen,[2] Emily L. Schaller,[3] Michael E. Brown,[3] Bonnie J. Buratti,[2] Christophe Sotin,[4] Caitlin Griffith,[1] Roger Clark,[5] Jason Perry,[1] Stephanie Fussner,[1] John Barbara,[6] Richard West,[2] Charles Elachi,[2] Antonin H. Bouchez,[7] Henry G. Roe,[3] Kevin H. Baines,[2] Giancarlo Bellucci,[8] Jean-Pierre Bibring,[9] Fabrizio Capaccioni,[10] Priscilla Cerroni,[10] Michel Combes,[11] Angioletta Coradini,[8] Dale P. Cruikshank,[12] Pierre Drossart,[11] Vittorio Formisano,[8] Ralf Jaumann,[13] Yves Langevin,[9] Dennis L. Matson,[2] Thomas B. McCord,[14] Phillip D. Nicholson,[15] Bruno Sicardy[11]

Observations from the Cassini Visual and Infrared Mapping Spectrometer show an anomalously bright spot on Titan located at 80°W and 20°S. This area is bright in reflected light at all observed wavelengths, but is most noticeable at 5 microns. The spot is associated with a surface albedo feature identified in images taken by the Cassini Imaging Science Subsystem. We discuss various hypotheses about the source of the spot, reaching the conclusion that the spot is probably due to variation in surface composition, perhaps associated with recent geophysical phenomena.

Large-scale relatively bright and dark regions are present on Titan's surface. Two bright areas particularly stand out: the continent-sized Xanadu Regio centered at 110°W, 15°S and the sub-Saturnian mid-south-latitude bright region (now provisionally named "Tsegihi")

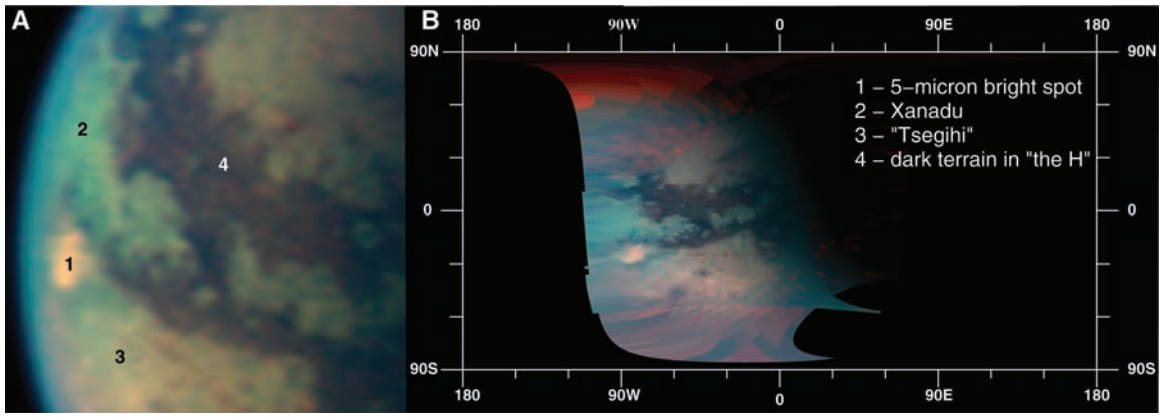

Fig. 1. Global image view (**A**) and cylindrical map view (**B**) of T5 (16 April 2005) data showing the spot. These color (but not true color) composites were created using data from the 1.57-μm atmospheric window as blue, from the 2.0-μm atmospheric window as green, and from the 5-μm atmospheric window as red. The area labeled 1 indicates the area from which we obtained bright spot spectra. 2 indicates Xanadu, 3 the sub-Saturnian mid-south-latitude bright region "Tsegihi," and 4 the area representing dark terrain. Areas 1, 2, and 3 were chosen to have broadly similar emission angles and atmospheric contributions.

centered at 15°W, 40°S. Several groups (*1*–*3*) have hypothesized that dark organic haze particles settling out of the atmosphere might build up all over Titan's surface, only to be washed away during methane rainstorms; thus, the bright areas would be composed of dirty ice (*4*) and the dark areas would be covered by organics. Other Earth-based observations have showed evidence for lakes of liquid hydrocarbon (*5*) along with methane clouds (*6*). Hence, Titan may be the only object other than Earth that is known to have an active exchange of liquid between the atmosphere and surface.

Three Cassini instruments can see through the haze in Titan's atmosphere. The Visual and Infrared Mapping Spectrometer (VIMS) uses spectral image mapping to obtain images in 352 colors simultaneously (*7*). VIMS's wavelength range, 0.3 to 5.2 μm, includes spectral windows at 0.92, 1.06, 1.26, 1.57, 2.0, 2.7, and 5.0 μm, where neither haze nor atmospheric absorption completely obscures the surface. The Imaging Science Subsystem (ISS) is a visible/near-infrared (IR) camera with a charge-coupled device detector (*8*). ISS is capable of observing Titan's surface through its 0.938-μm filter. Cassini's radar radiometer investigates spatial variation in surface properties with both active and passive modes. At short range, the radar is operated in active mode as a 2.17-cm synthetic aperture radar (*9*). At larger ranges, it can operate in passive mode, measuring the microwave flux from Titan's surface.

Here we present observations of an unusual bright region on Titan, southeast of Xanadu. The bright spot is located at 80°W, 25°S and became apparent in adaptive optics 1.6-μm (*10*) and 2.0-μm imaging from the Keck Observatory. VIMS obtained its best views of the area on 31 March 2005 (T4) and 16 April 2005 (T5) (Fig. 1). A bright area consistent with this one is also present in data taken on 2 July 2004 (T0), 26 October 2004 (TA), and 13 December 2004 (TB), (Fig. 2). Thus, the spot was observed consistently over 9 months. The spot was near the sub-solar point during T5, but the spacecraft trajectory limited views of the spot to emission angles of over 60° at a spatial resolution of 30 km per pixel in the north/south direction

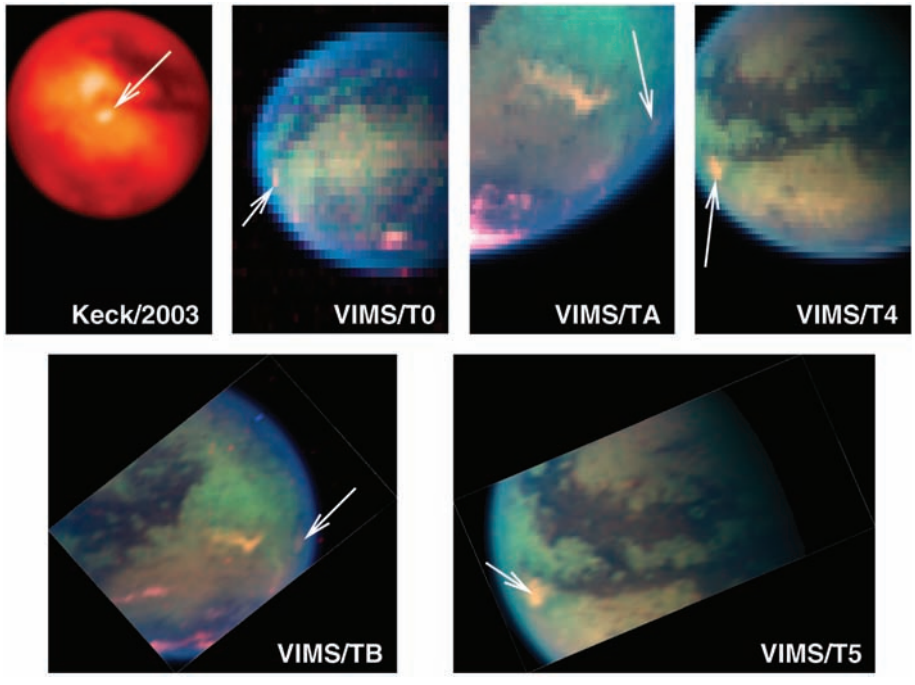

Fig. 2. Identifications of the 5-μm-bright spot from Keck AO ground-based imaging on 24 December 2003 and from VIMS during Cassini encounters on 3 July 2004 (T0), 26 October 2004 (TA), 13 December 2004 (TB), 31 March 2005 (T4), and 16 April 2005 (T5). North is at the top in all images. Keck data were taken through the K′ filter (1.95 to 2.30 μm) and color-mapped to produce the upper left image. The VIMS images were generated with 5 μm (VIMS channels 337 to 362 added together) as red, 2.0 μm as green, and 1.57 μm as blue. Spectral coverage for the T0 encounter was limited by bandwidth constraints; for the T0 image, we scaled the available data to simulate the full spectral window coadditions that were used in the other flybys. The 5-μm-bright spot shows no spectral or spatial changes between T4 and T5, although the geometry of the other encounters is poor enough to not rule out changes in spatial coverage.

[1]Lunar and Planetary Laboratory, University of Arizona, Tucson, AZ 85721, USA. [2]Jet Propulsion Laboratory, California Institute of Technology, Pasadena, CA 91109, USA. [3]Geological and Planetary Sciences, California Institute of Technology, Pasadena, CA 91125, USA. [4]Laboratoire de Planétologie et Géodynamique, UMR CNRS 6112, Université de Nantes, France. [5]U.S. Geological Survey, Flagstaff, AZ 86001, USA. [6]NASA Goddard Institute for Space Studies, New York, NY 10025, USA. [7]W. M. Keck Observatory, Kamuela, HI 96743, USA. [8]Istituto di Fisica dello Spazio Interplanetario, Consiglio Nazionale delle Richerche, Rome 00133, Italy. [9]Institut d'Astrophysique Spatiale, Université de Paris-Sud, Orsay 91405, France. [10]Istituto di Astrofisica Spaziale e Fisica Cosmica, Consiglio Nazionale delle Richerche, Rome, Italy. [11]Observatoire de Paris, Meudon, France. [12]NASA Ames Research Center, Moffet Field, Mountain View, CA 94035–1000, USA. [13]Institute of Planetary Exploration, German Aerospace Center, Berlin 12489, Germany. [14]Department of Earth and Space Sciences, University of Washington, Seattle, WA 98195–1310, USA. [15]Department of Astronomy, Cornell University, Ithaca, NY 14853, USA.

*To whom correspondence should be addressed. E-mail: jbarnes@lpl.arizona.edu.

and 150 km per pixel in the east/west direction. Resolution was similar during T4. The spot's morphology was the same during both encounters. These observations are, therefore, consistent with a static feature.

The 5-μm-bright spot extends 450 km from north to south and 400 km from Titanian west to Titanian east. It is brightest in the mid-north. The spot is brighter than conventional bright terrain at all wavelengths, and it becomes progressively brighter than Xanadu beyond 1.6 μm (Fig. 3). In images created by co-adding all of the VIMS frames in the 5-μm spectral window, the spot outshines the sub-Saturnian mid-south-latitude bright region ("Tsegihi") by 17% and outshines Xanadu by nearly a factor of 2. The spot's spectral signature more closely resembles that of "Tsegihi" than that of Xanadu; even though the spot might spectrally be yet-brighter "Tsegihi" terrain, Xanadu's sharply lower albedo at 5 μm is distinct. At 2.65 μm, the spot is of similar intensity relative to incoming solar flux (*I*/*F*) relative to other bright terrain, but is ~15% brighter than other terrain at 2.75 μm.

A thin, bright, semicircular feature bounded the 5-μm-bright spot to the south, as seen by ISS in December 2004 (TB). This feature ("the Smile") is 650 km long and up to ~90 km wide. The arc does not continue to the north, so it does not mark a recent circular impact structure. It could be a heavily eroded crater, although the old crater idea does not explain why "the Smile" is so bright. The feature's symmetry seems to imply structural control. The ISS image shows a crenulated margin, perhaps due to surface flows or erosion. ISS also observed this region in February 2005 (T3) and, within the limits of resolution, no difference in "the Smile" was detected.

"The Smile" is brighter than the rest of Xanadu (Fig. 4b). In the region where the 5-μm flux is strongest (the area within or bounded by "the Smile"), ISS shows a 300 × 500 km area of high albedo trending northeast-southwest. The 0.938-μm albedo of this area is comparable to that in Xanadu. Therefore, the 0.938-μm and 5.0-μm albedos of this area interior to "the Smile" are not correlated (Fig. 4C). In contrast, the albedos measured elsewhere on the surface of Titan by ISS and VIMS correlate strongly.

A moderately bright 0.938-μm area underlies the triangular tongue that is bright at 5 μm and stretches toward the southwestern edge of the H-shaped dark region that was first seen from Earth (*11*). But to the northwest, areas that are somewhat bright at 5.0 μm overlie a region that is dark at 0.938 μm. This variation probably reflects resolution differences between the two data sets. Thin, bright, radial fingers extend northward from "the Smile"'s center of arc into the dark region in the ISS view. The superposition of the bright fingers and dark background probably results in the moderate 5-μm brightness detected by VIMS. If this interpretation is correct, then the increased 5-μm flux is correlated with ISS bright terrain.

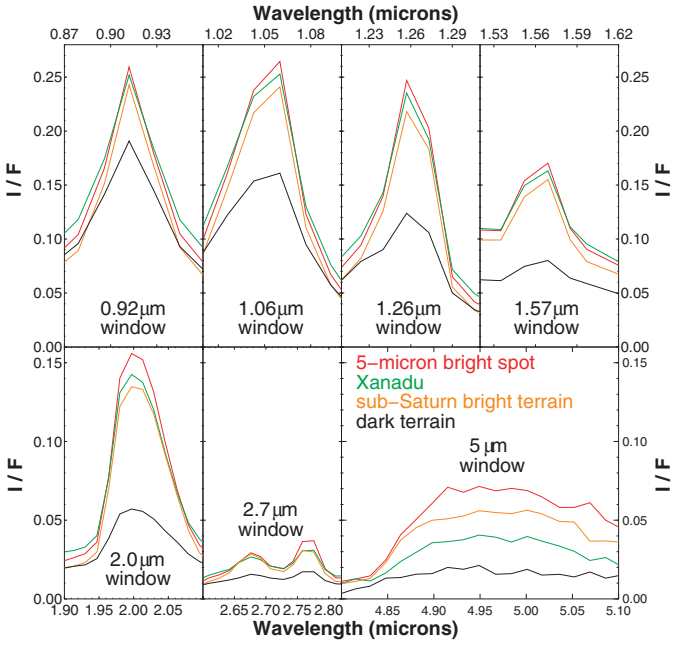

Fig. 3. Spectral comparison of the spot, Xanadu, the sub-Saturnian mid-south-latitude bright region ("Tsegihi"), and dark terrains within Titan's different spectral windows. All Titanian bright terrain is not the same: Xanadu and "Tsegihi" are distinctly different from one another. Although Xanadu is brighter than "Tsegihi" at wavelengths shorter than 5 μm, it is dimmer at 5 μm, which may imply an icier composition. The bright spot more closely tracks Xanadu in its overall brightness, but like "Tsegihi" is much brighter than Xanadu at 5 μm.

A low-resolution passive radiometry observation from T4 covers the study area (Fig. 4D) in one polarization, with a spatial resolution of about 250 km. A correlation of higher brightness temperature with lower near-IR albedo in the upper right corner of the map is prominent. This correlation appears to hold for most of Titan's surface at these spatial scales.

The spot cannot be specular reflection because the specular point for flat surfaces was located thousands of kilometers to the east. VIMS's observations span 12° to 57° in phase angle and show no variation in the spectral character of the spot; the much better-sampled ground-based Keck adaptive optics (AO) observations of the spot also show that its phase function matches the surrounding terrain between 0° and 70°.

The low density of craters on Titan (*12*, *9*) implies a high resurfacing rate that may involve cryovolcanism (*9*). We performed radiative simulations that show the bright spot's 5-μm excess to be consistent with roughly gray-body thermal emission at a temperature of ~180 K. Some features of the ISS morphology are consistent with the idea that the 5-μm-bright spot represents a volcanic province: the bright optical albedo, crenulated margins, and possible linear flow features.

To test this hypothesis, we calculated brightness temperatures from passive microwave radiometry obtained by Cassini's radar during the T4 encounter. The microwave brightness temperature depends on polarization, incidence angle, composition, and physical temperature (*13*). The observations in Fig. 4D were made at incidence angles of around 57°, close to the Brewster angle for ices and hydrocarbons. At this angle, vertically polarized radiation is perfectly absorbed or emitted by the surface, and thus (in the absence of subsurface scattering) the brightness temperature corresponds exactly to the physical temperature. Our observation with an antenna temperature of ~77 K had the polarization vector about 38° from vertical, which represents a sum of horizontal and vertically polarized brightness temperatures weighted (~62%) in favor of the vertical. Application of the orthogonal polarization, lower-resolution radiometer data (71 K) also taken on T4 suggests vertical brightness temperature $T_b(V) \sim 83$ K and horizontal brightness temperature $T_b(H) \sim 67$ K. The vertically polarized value is rather typical for other regions on Titan and is lower than the thermodynamic temperature of the surface because of subsurface scattering (which in effect partly reflects cold sky into the instrument in place of some surface emission). There is thus no evidence for elevated surface temperatures, which rules out the hot spot hypothesis.

If the spot represents a topographic high, sunlight would pass through less of Titan's atmosphere both incoming from the Sun and outgoing to Cassini. The reduced path length through the atmosphere would decrease both scattering by haze particles and absorption by atmospheric gases, resulting in a higher observed *I*/*F* for a surface of a given albedo. Because the optical depth of Titan's haze decreases with increasing wavelength, this hypothesis has difficulty explaining the spot's high 5-μm brightness. In addition, the lack of a strong negative brightness temperature anomaly associated with the feature in radiometry appears to argue against its being substantially elevated above surrounding areas. With a dry adiabatic lapse rate of ~0.6 to 0.8 K/km, even a generous 1 to 2 K temperature drop would

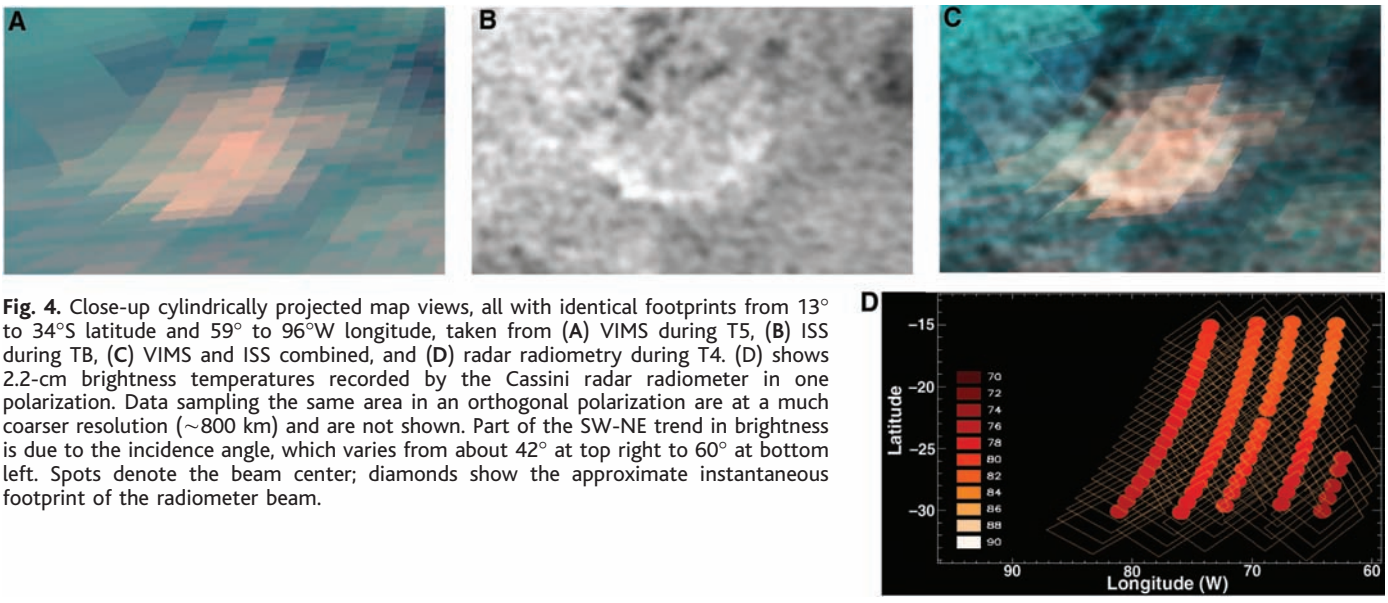

Fig. 4. Close-up cylindrically projected map views, all with identical footprints from 13° to 34°S latitude and 59° to 96°W longitude, taken from (**A**) VIMS during T5, (**B**) ISS during TB, (**C**) VIMS and ISS combined, and (**D**) radar radiometry during T4. (D) shows 2.2-cm brightness temperatures recorded by the Cassini radar radiometer in one polarization. Data sampling the same area in an orthogonal polarization are at a much coarser resolution (~800 km) and are not shown. Part of the SW-NE trend in brightness is due to the incidence angle, which varies from about 42° at top right to 60° at bottom left. Spots denote the beam center; diamonds show the approximate instantaneous footprint of the radiometer beam.

permit only 3 km of topography, which is not enough to account for the spot's brightness.

Two major lines of reasoning, however, argue against this feature being a cloud. First, the spot's spectrum does not match that of known clouds; second, the feature has persisted for much longer than known clouds. The uniformly high inferred albedo for the spot across VIMS's entire spectral range is consistent with cloud particles. If the 5-μm-bright spot is caused by methane condensate, it would have to be in the form of a persistent low-lying cloud or ground fog.

Keck and Cassini observations have found this particular spot to be bright and to maintain its spatial distribution for 4.5 years. Clouds seen in the past formed and dissipated on time scales between hours and days. With better spatial resolution and higher time resolution, ISS monitoring of this region during TB showed no apparent changes over tens of hours. If the spot is a cloud, it must be a cloud that is tightly controlled by the surface. It could be orographic, but on Earth and Mars, even though orographic clouds appear preferentially in certain places, they still appear, disappear, and change shape over time. The spot could correspond to fog overlying a lake, hot springs, or a volcanic field. However, the higher-altitude clouds that we have seen so far are much brighter than Xanadu when viewed by ISS, and although "the Smile" meets this criterion, the interior of the 5-μm-bright spot does not.

Finally, the 5-μm-bright region may be the result of a surface albedo marking. As such, it could represent an area with distinct crustal composition, an area in an unusual state of weathering, or a thin surficial coating. Because water ice is highly absorbing at 5 μm, the 5-μm-bright area cannot be more water-rich than either Xanadu or the sub-Saturnian mid-south-latitude bright region "Tsegihi." The strong negative deviation of Xanadu's spectrum at 5 μm implies that it is Xanadu that has more water ice than either the bright spot or "Tsegihi." It is not obvious what composition might be both brighter than Xanadu at long wavelengths where water absorbs and brighter at short wavelengths where water strongly reflects. The area could be in an unusual state of weathering—either very young geologically or perhaps just recently cleaned by methane rainfall. Either might alter the chemistry of the topmost surface layer in a manner that could reproduce the observed spectrum, although it would seem that a recent methane cleaning would leave the area more icy, not less. Finally, the spatially localized nature of the 5-μm excess could be the result of a thin airfall deposit, perhaps emanating from vents in "the Smile" and blown northeast by prevailing winds. However, it is still difficult to conceive of a substance with the right spectral properties.

If the radiometric brightness temperatures $T_b(\mathrm{V}) \sim 83$ K and $T_b(\mathrm{H}) \sim 67$ K are interpreted as due to emission from a dielectric surface at 83 K (thus taking subsurface scattering crudely into account), the ratio of the two temperatures suggests a dielectric constant of ~3. This value is rather higher than that typical for Titan as a whole, which exhibits polarization that is characteristic of dielectric constants of 2. The value would be consistent with the study area having an ice-rich composition, in contrast to the widespread value characteristic of porous ices or solid or liquid hydrocarbons. Pure ice appears inconsistent with the VIMS data. However, because the absorptivity or loss tangent of cold ice and hydrocarbons is very low ($< \sim 10^{-4}$), the microwave data probe depths of perhaps several meters. Hence, a thin frost or veneer of material only a few tens of microns thick could give the surface a very different near-IR reflectance from that expected from its bulk composition.

An intriguing possibility for the identity of the bright spot's reflecting material is CO_2 ice. CO_2 ice reflects highly in the same short-wavelength Titanian atmospheric windows where water ice reflects, but is more highly reflective than water ice in the 5-μm window. Unfortunately, the most diagnostic wavelengths for carbon dioxide ice are not within Titan's spectral windows and thus are not amenable to remote sensing. Kress and McKay (*14*) recently predicted an abundance of CO_2 on Titan, based on chemical modeling of comet impacts early in Titan's history. In this scenario, the bright spot and "Tsegihi" could be either eroded layers of CO_2 or more recent overlying deposits. Observations in the coming years will shed additional light on this enigmatic feature.

References and Notes

1. C. A. Griffith, T. Owen, R. Wagener, *Icarus* **93**, 362 (1991).
2. J. I. Lunine, *ESA SP-338: Symposium on Titan* (European Space Agency, 1992), pp. 233–239.
3. P. H. Smith *et al.*, *Icarus* **119**, 336 (1996).
4. C. A. Griffith, T. Owen, T. R. Geballe, J. Rayner, P. Rannou, *Science* **300**, 628 (2003).
5. D. B. Campbell, G. J. Black, L. M. Carter, S. J. Ostro, *Science* **302**, 431 (2003).
6. C. A. Griffith, T. Owen, G. A. Miller, T. Geballe, *Nature* **395**, 575 (1998).
7. R. H. Brown *et al.*, *Icarus* **164**, 461 (2003).
8. C. C. Porco *et al.*, *Space Sci. Rev.* **115**, 363 (2004).
9. C. Elachi *et al.*, *Science* **308**, 970 (2005).
10. H. G. Roe *et al.*, *Geophys. Res. Lett.* **31**, 17 (2004).
11. M. Hartung *et al.*, *Astron. Astrophys.* **421**, L17 (2004).
12. C. C. Porco *et al.*, *Nature* **434**, 159 (2005).
13. R. D. Lorenz *et al.*, *Planet. Space Sci.* **51**, 353 (2003).
14. M. E. Kress, C. P. McKay, *Icarus* **168**, 475 (2004).
15. Some of the data presented herein were obtained at the W. M. Keck Observatory, which is operated as a scientific partnership among the California Institute of Technology, the University of California, and NASA. The observatory was made possible by the generous financial support of the W. M. Keck Foundation. This work was funded by the Cassini project. Authors from U.S. institutions were funded by NASA; authors from European institutions were funded by the European Space Agency.

7 July 2005; accepted 9 September 2005
10.1126/science.1117075